

PROCEEDINGS OF SPIE

SPIDigitalLibrary.org/conference-proceedings-of-spie

Modeling and experimental investigation of transverse mode dynamics in VECSEL

Alexandre Laurain, Jorg Hader, Jerome V. Moloney

Alexandre Laurain, Jorg Hader, Jerome V. Moloney, "Modeling and experimental investigation of transverse mode dynamics in VECSEL," Proc. SPIE 10901, Vertical External Cavity Surface Emitting Lasers (VECSELs) IX, 109010C (4 March 2019); doi: 10.1117/12.2510281

SPIE.

Event: SPIE LASE, 2019, San Francisco, California, United States

Modeling and experimental investigation of transverse mode dynamics in VECSEL

Alexandre Laurain, Jorg Hader, and Jerome V. Moloney.

College of Optical Sciences, University of Arizona, Tucson, AZ 85721.

ABSTRACT

We present a new method to simulate the formation of transverse modes in VECSELs. An expression for the gain as a function of carrier density and temperature is derived from a simulation of the structure reflectivity, while the field propagation in the cavity is computed with the Huygens-Fresnel integral. A rate equation model is employed to calculate the field and gain dynamics over numerous round-trips. The optimal mode size for single mode operation for a given pump shape is calculated and compared to experimental results. The effect of pump geometry, thermal lensing and structure design will be discussed.

Keywords: VECSEL, OPSL, semiconductor, Transverse modes, dynamics.

Introduction

Thanks to their external cavity and circular symmetry, optically-pumped VECSELs provide high output power with high quality TEM₀₀ mode. Unlike with other semiconductor lasers, like edge emitters diodes or VCSELs, the laser beam of a VECSEL doesn't propagate in a waveguide but in free space and will thus be subject to diffraction. This feature has many advantages, one of which is the possibility to freely adjust the fundamental mode size of the laser cavity by choosing the adequate cavity geometry and focusing elements (mirror, lenses). This means that the cavity can be designed to give a very large fundamental mode size (>1 mm), which is key to power scalability. Furthermore, the possibility to adjust the overlap between the fundamental mode and the pump beam enables single mode operation with very large modes as higher order mode are eliminated through spatial filtering in the gain medium. In contrast, the transverse dimension of a single mode waveguide is usually limited to a few wavelengths (V-parameter), i.e. a few μm , which strongly limit the available output power and highly increase the beam divergence. As most semiconductor laser, the power performance of a VECSEL is limited by the pump-induced heating of the gain medium. But since it is possible to scale the pump diameter to reduce the thermal impedance of the device, high power single mode operation can be achieved. Indeed, increasing the beam diameter in the VECSEL reduces the thermal impedance as it distributes the pump induced heat over a larger beam area leading to lower temperature rises. It also reduces the optical power density, hence increasing the laser induced damage threshold. This power scaling method, combined with an efficient thermal management technology (substrate removal, diamond bonding, etc) yielded to record power from a single semiconductor device,¹ and high brightness highly coherent emission.^{2,3,4} However, despite these experimental successes, it is still not clear what is the optimal mode size ratio between the fundamental mode and the pump beam, giving the maximum power in the fundamental mode with the highest beam quality. This optimum for a given VECSEL setup is not explicit, and to our knowledge has not been investigated theoretically.

To evaluate the transverse modes discrimination in VECSELs, one might think that the calculation of an overlap function between the pump beam and the different cavity modes would provide a good approximation. But such approach is flawed as it doesn't account for gain saturation, spatial hole burning effects, beam distortion, diffraction losses, etc. A more adequate approach is to simulate the full dynamic of the transverse mode formation in a self-consistent way.

Here, we present a system-oriented spatio-temporal model to simulate the formation of transverse modes in VECSELs. In the first section we give an analytical expression for the gain as a function of the carrier density and temperature which is derived from a simulation of the full structure reflectivity. Then, we simulate the

Further author information: (Send correspondence to A. Laurain)

A. Laurain: E-mail: alaurain@optics.arizona.edu

Vertical External Cavity Surface Emitting Lasers (VECSELs) IX, edited by
Ursula Keller, Proc. of SPIE Vol. 10901, 109010C · © 2019 SPIE
CCC code: 0277-786X/19/\$18 · doi: 10.1117/12.2510281

temperature profile in the active structure for two of the most common pump shapes using a finite element method. The result is subsequently fitted with a polynomial equation to provide an analytical expression for the temperature. In a second section, we present a numerically optimized method to calculate the field propagation in the VECSEL cavity using a one step Huygens-Fresnel integral. In the third section, we present the full model employed to calculate the field and gain dynamics over numerous round-trips. Some simulation results we be given in the last section, where we will discuss the effect of the pump shape, pump power, output coupler, structure design on the steady state solution of the transverse mode which will define the laser performance in CW operation.

1. SPATIAL GAIN OF A VECSEL STRUCTURE

1.1 Structure design

For this paper we will consider a VECSEL structure grown on a GaAs wafer for an emission wavelength at 1000 nm. We will also focus on a structure designed for high power CW operation, which typically has a Resonant Periodic Gain (RPG) active region, where the active medium consists of InGaAs quantum wells (QWs) placed periodically on the antinodes of the standing wave field. The structure simulated here consists of a half wavelength InGaP confinement/cap layer, followed by an active region containing 10 InGaAs QWs placed uniformly on each antinodes of the field and surrounded by pump-absorbing GaAs(P) barriers. The structure is terminated with a 22 pairs high-reflectivity AlAs/AlGaAs Distributed Bragg Reflector (DBR), transparent at the pump wavelength of 808 nm, and soldered onto a diamond heatspreader. A similar structure design was previously used to demonstrate above 15 W in single frequency operation⁵ and above 100 W in multimode operation.¹ The structure may also be coated with a single layer of silicon nitride, which is typically used to minimize the surface reflection at the signal and pump wavelength and to provide a wider gain bandwidth or tunability.

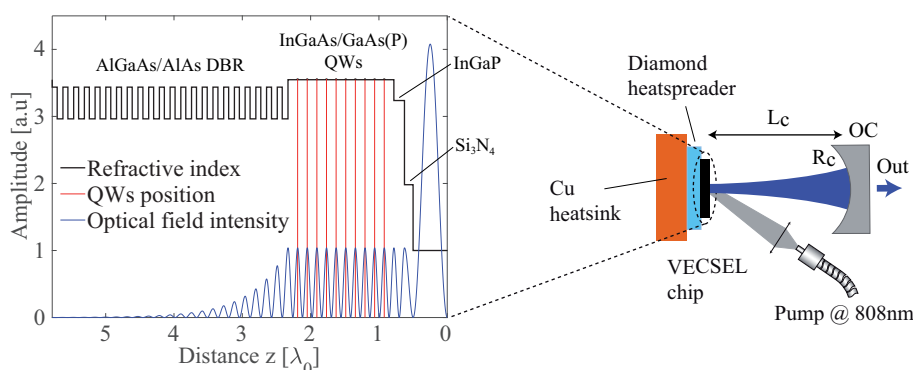


Figure 1. Schematic layout of the simulated VECSEL structure and typical VECSEL setup in a linear cavity.

1.2 Gain calculation

The gain of a VECSEL structure doesn't only depend on the material gain (QW) but also depends on the field enhancement factor of the structure as well as the DBR reflectivity, all of which are also temperature dependent. Therefore, to account for all these effects, we simulated the full structure reflectivity as a function of the temperature and carrier density, using standard matrix transfer methods. The material gain was computed at various carrier density and temperature values using a microscopic approach based on the semiconductor Bloch equation, which is described in Ref.⁶ and the references therein. This gain database is also available with the software SimuLaseTM. The structure is designed such that at room temperature the QW gain peak wavelength is blue-shifted relative to the microcavity resonance in order to reach a perfect alignment at high temperature (375K) i.e. at high pump power. Once the reflectivity spectra are computed, we evaluate the gain value at the nominal lasing wavelength. These gain values are then fitted with a 2D polynomial function of the fifth order with the parameters N and T . Fig. 2 shows the simulated gain at 1000nm as a function of the carrier density and temperature together with the fitted polynomial. This gives an analytical expression for the gain as a function of the carrier density and temperature which can then be used for the transverse mode dynamic simulation, minimizing the computing load significantly.

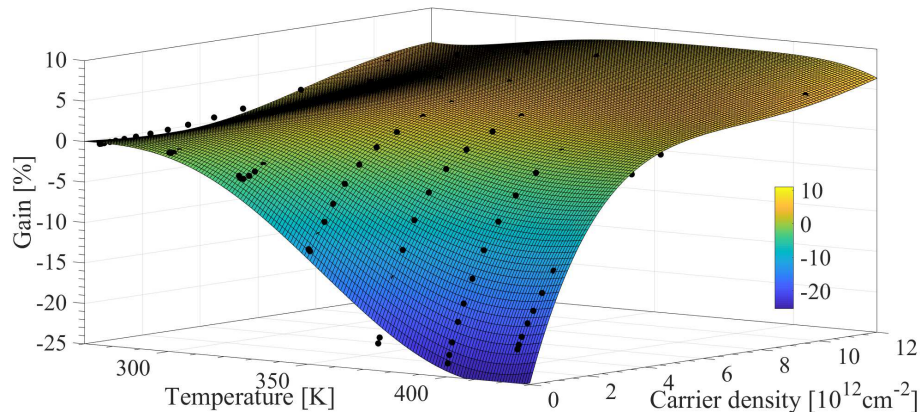


Figure 2. Points: Simulated gain value of an AR-coated VECSEL structure at 1000 nm as a function of temperature T and carrier density N . Surface curve : fitted 2D polynomial function.

1.3 Simulated temperature profile

Since the spatial gain profile in an optically pumped VECSEL structure is mostly defined by the spatial distribution of the pump beam, it is important to evaluate the temperature profile for a given pump beam shape (Gaussian, super-Gaussian, etc). Here, we will consider two of the most common pump beam shapes: a gaussian beam with a waist of $175 \mu\text{m}$, and a supergaussian beam of order 25 with the same waist parameter of $175 \mu\text{m}$. The temperature distribution induced by such pump shapes were simulated using a finite elements method (Comsol MultiphysicsTM). The transverse temperature profile on each QW is then averaged along the active region and fitted with a polynomial function. The results of these simulations are shown on Fig. 3.

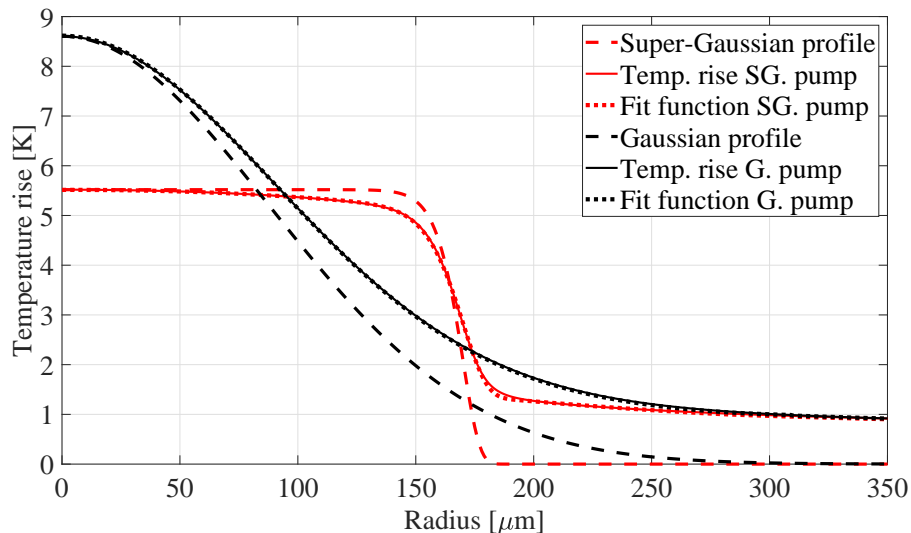


Figure 3. Simulated transverse temperature profiles with a Supergaussian (SG) and Gaussian (G) pump shapes, assuming a pump induced heating of 1 W in the RPG region. The pump profiles normalized to the max temperature are also plotted for comparison.

1.4 Spatial gain

With an analytical function for the gain as a function of the carrier density and an analytical function for the temperature as a function of the transverse dimension, we can calculate the spatially dependent gain of the VECSEL structure for a given pump shape and power. We will assume that the carrier density follows the pump intensity distribution as the carrier diffusion length ($\sim 1\text{-}2\mu\text{m}$) is negligible compared to the dimensions of the

pump beam considered here. Some gain profiles calculated at various pump power for an AR-coated structure are shown on Fig. 4.

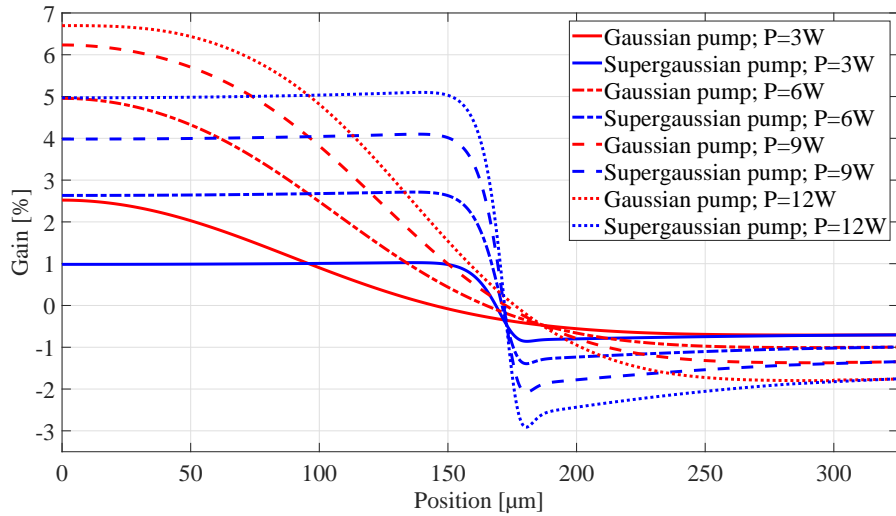


Figure 4. Simulated gain profile of a VECSEL structure with a Supergaussian (SG) and Gaussian (G) pump shapes at various level of absorbed pump power.

2. ROUND-TRIP MODE PROPAGATION IN VECSEL CAVITIES

Since most VECSEL cavities do not contain hard apertures and the lasing beam has low to very low divergence, the optical field propagation can be accurately described in the paraxial approximation. The simplest cavity geometry is of course the linear cavity with the VECSEL structure at one end and a curved output coupler mirror at the other end, separated by an air gap of a few millimeters to a few centimeters. Even with such simple cavity, one must account for the the propagation of the field from one end to the other, a spatial phase transformation for the curved mirror and another propagation to complete a round trip. If the cavity geometry is more complex, like with a V-shaped or Z-shaped cavity for example, the number of propagation and transformation increases significantly, which is a numerical burden for the computation of the transverse mode dynamic. However, a very useful form of paraxial optics theory has been developed to handle not only propagation in free space, but also in more general types of paraxial systems. If we consider a paraxial optical system that can be described with an ABCD matrix such as a VECSEL cavity for example (Fig. 5), it is possible to calculate the total Huygens' integral of the system in one step, using only the overall ABCD matrix of the cascaded optical elements.

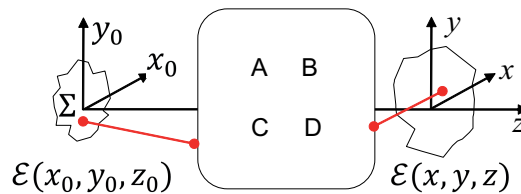


Figure 5. Schematic of a field propagation through a paraxial optical system described by its ABCD matrix.

In the case of a round-trip calculation, the input plane is evidently the same as the output plane. If we simplify the system to one transverse dimension, the Huygens' integral for propagation through the entire cavity (full round trip propagation) is given by:⁷

$$\mathcal{E}(r) = e^{-jkL_0} \sqrt{\frac{j}{B\lambda}} \int e^{-j\frac{\pi(Ar_0^2 - 2rr_0 + Dr^2)}{B\lambda}} \mathcal{E}(r_0) dr_0 \quad (1)$$

Where $\mathcal{E}(r_0)$ is the complex field at the transverse location r_0 in initial plane located at z_0 , $L_0 = z - z_0$ is the total round trip propagation length ($L_0 = 2L_c$ for a linear cavity of length L_c), λ is the wavelength in free space. Furthermore, for computation efficiency, it is possible to use a coordinate transformation with a 'collimated Fresnel number' to express this integral in a form allowing fast Fourier transform methods.⁷ This powerful numerical method greatly reduces the computation load, as only a coordinate transformation and a fast Fourier transform are necessary for the mode propagation over a complete round trip. This allows calculation with high spatial resolution over numerous cavity round trips with a standard computer.

3. TRANSVERSE MODE DYNAMICS MODEL

Now that we have an analytical model for the spatial gain profile of the active structure and an efficient mode propagation method, it is possible to simulate the transverse mode dynamics of a given VECSEL cavity. A schematic representation of the general algorithm used for the simulation of the transverse mode dynamics is presented on Fig. 6.

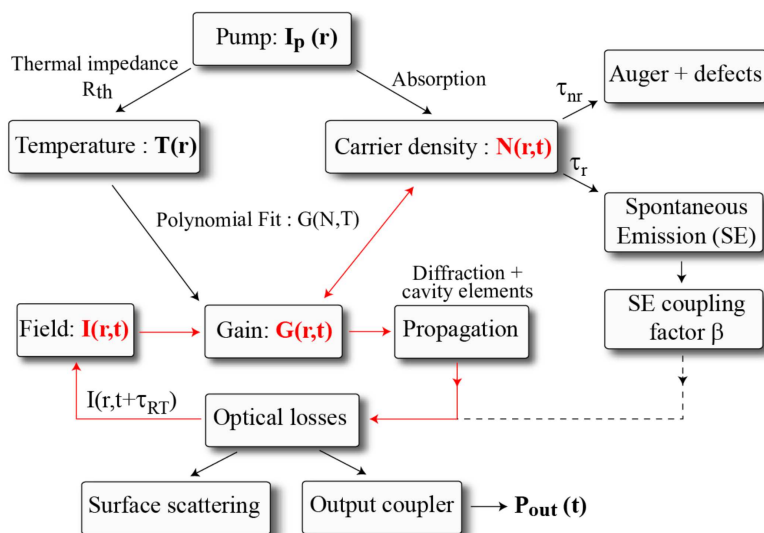


Figure 6. Schematic representation of the model used for the simulation of the transverse mode dynamics.

The laser rate equations approximation are used to describe the field-matter interaction and the propagation of the field is handled with the generalized Huygens' integral presented previously. This integral is calculated at time intervals corresponding to the round-trip time τ_{RT} , while the differential equations is evaluated at a smaller time interval to ensure numerical accuracy. We will assume that the lasing mode is linearly polarized, as it is generally observed with VECSELs exhibiting a slight gain dichroism or Brewster plate in the cavity.^{5,8} The set of equations describing the system is thus given by:

$$\frac{dN(r,t)}{dt} = \frac{\lambda_p I_p(r)}{hcN_{qw}} - \frac{N(r,t)}{\tau_e} - \frac{\lambda_l}{hcN_{qw}} |\mathcal{E}(r,t)|^2 \times G(r,t) \quad (2)$$

$$\frac{d\mathcal{E}(r,t)}{dt} = \frac{G(r,t) - OC}{2\tau_{RT}} \mathcal{E}(r,t) \quad (3)$$

$$\mathcal{E}(r, m\tau_{RT}) = \text{Huygens} \left\{ \mathcal{E}(r, m\tau_{RT}) \times e^{-jk_0 n(r) \Gamma L_{\mu c}} \right\} \quad (4)$$

$$\text{with } G(r,t) = \text{Poly2D} [N(r,t), T(r)] \quad (5)$$

$$\text{and } n(r) = n_0 + \frac{\partial n}{\partial T} [T(r) - T_0] + \frac{\partial n}{\partial N} [N(r,t) - N_0] \quad (6)$$

Where λ_p and I_p are respectively the pump wavelength and pump power density. N_{qw} is the number of QW in the structure, τ_e is the effective carrier lifetime, and OC the output coupling loss. The phase term in eq. (4) reflects the refractive index variation $n(r)$ within the semiconductor structure microcavity. The product of the longitudinal confinement factor Γ by the microcavity length $L_{\mu c}$ represents the total optical path length of the field in the structure. The first term of eq. (6) is the average refractive index of the semiconductor evaluated at $T = T_0$ and $N = N_0$, the second term represents the thermal lensing, whereas the third term represent the carrier induced refractive index change. This last term is usually an order of magnitude smaller than the thermal lensing effect, and will therefore be neglected. The thermal lensing is however not always negligible, and in some cases is the dominant mechanism for the confinement of transverse modes, such as with a short plano-plano VECSEL cavity.²

4. RESULTS

To mimic the initial spontaneous emission, the field is initialized with an intensity distribution following the pump shape with an intracavity average power of 0.1 mW. The field is propagated in the cavity for 15000 round-trips or until a steady state is reached. The cavity geometry simulated is a linear cavity composed of the gain structure and a concave output coupler mirror separated by an air gap of 50 mm. At first, the output coupling losses are kept constant at $OC = 3\%$, whereas the radius of curvature R_c is varied to obtain different fundamental mode sizes. Since we are mostly interested on the steady state solution of the system, we will give the final output power of the system together with the beam quality factor M^2 of the laser.

4.1 Output power vs. mode size ratio

The purpose of this simulation is to investigate the effect of the beam size ratio between the fundamental mode of the cavity and the pump beam to find the optimal ratio giving the maximum output power while keeping a high beam quality, i.e. the brightest mode. Fig. 7 shows the output power and the beam quality factor M^2 after 15000 round-trips as a function of the of mode/pump ratio for an AR-coated structure pumped with a super-Gaussian beam. The M^2 factor was obtained by calculating the second-moment beam width in the near field and far field, using the definition given in Ref.⁹

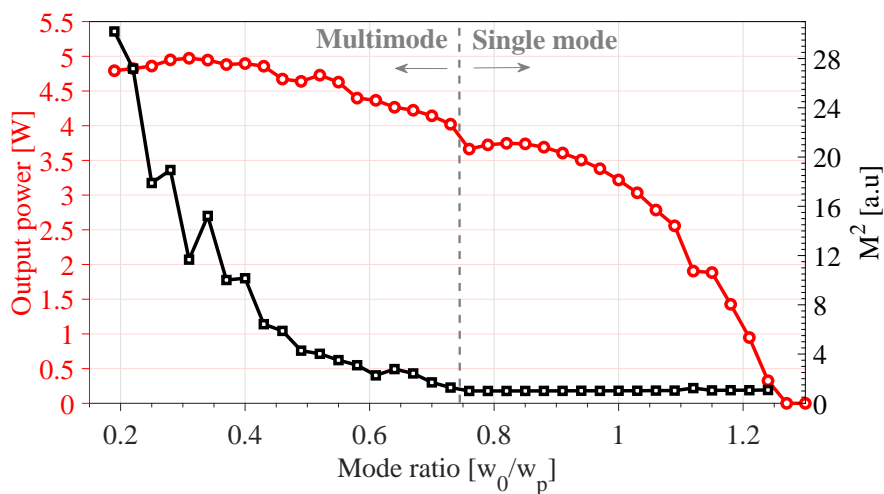


Figure 7. Simulated output power and beam shape quality factor M^2 after 15000 cavity round trips as a function of the mode/pump ratio. A super-Gaussian pump shape and an absorbed power of 18 W are assumed.

When the mode ratio is increased above 0.75, a clear transition between multimode and single mode operation occurs. The beam quality factor also decreases dramatically as less higher order modes are present, increasing the brightness of the output beam. In the single mode regime, the beam is nearly diffraction limited for all values of ratio ($M^2 \simeq 1$) and an optimum power seems to be reached when the ratio is about 0.82. At this value, the mode has a perfect balance between high saturation power and low absorption losses, and has a power about

25% lower than the maximum value of the multimode regime. This behavior is consistent with experimental observations where record average power were demonstrated with highly multimode cavities^{1,10} whereas single mode operation was obtained at the expense of a 30% power decrease when keeping the same pump size.¹⁰

4.2 Beam brightness vs. pump power

To study the influence of the pump power on the optimum ratio, we replicated the simulation presented previously at various pump powers. To give a more insightful characteristic of the laser beam, we plotted the optical brightness, which we define as the output power divided by the beam quality factor M^2 , as a function of the pump power and cavity mode size (Fig. 8).

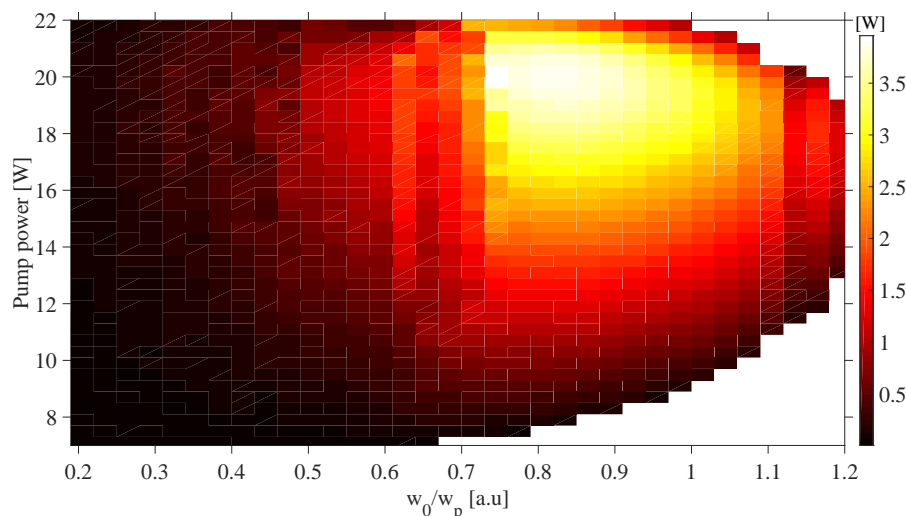


Figure 8. Simulated beam brightness after 15000 cavity round trips assuming a super-Gaussian pump shape.

Over the entire pump power range, the brightest mode is always obtained when the laser cavity supports only the fundamental TEM_{00} mode, and a transition between multimode and single mode operation occurs when the mode size ratio is increased above 0.75, with an optimum brightness of 3.87 W obtained at a ratio of 0.82 and a pump power of about 20 W. The transition occurs at a lower ratio when the pump power gets closer to threshold, as the modal gain of high order modes is no longer able to compensate for the absorption losses.

Now if we consider a Gaussian pump beam profile instead of a super-Gaussian shape, we can expect a different result since the temperature and gain profiles are much different. The optical brightness of a VECSEL pumped with a Gaussian pump beam is shown on Fig. 9.

The highest brightness is obtained at a lower mode ratio (~ 0.65) and at lower pump power (~ 14.5 W) as the thermal rollover occurs at an earlier stage due to the higher temperature rise at the center of the pump beam. The Gaussian pump profile is also more effective at filtering the higher transverse modes thanks to a significantly lower saturated gain far from the center. This simulation also shows that the optimum mode/pump size ratio increases with the pump power and the transition between multimode and single mode operation shifts toward higher mode/pump size ratio when the pump power increases. This is due to the spatial width of the net gain increasing with the pump power.

4.3 Optimum output coupler

To fully optimize the VECSEL cavity, the optimum output coupling needs to be determined. This search will be done at the optimum pump power (19 W for super-Gaussian pump), and the mode/pump size ratio will be varied to investigate its effect at the various OC value. Figure 10 shows the simulated beam brightness as a function of the output coupling losses and mode size ratio. For this calculation, we assumed 0.2% of scattering losses inside the cavity, which is a typical empirical value due to surface imperfections.

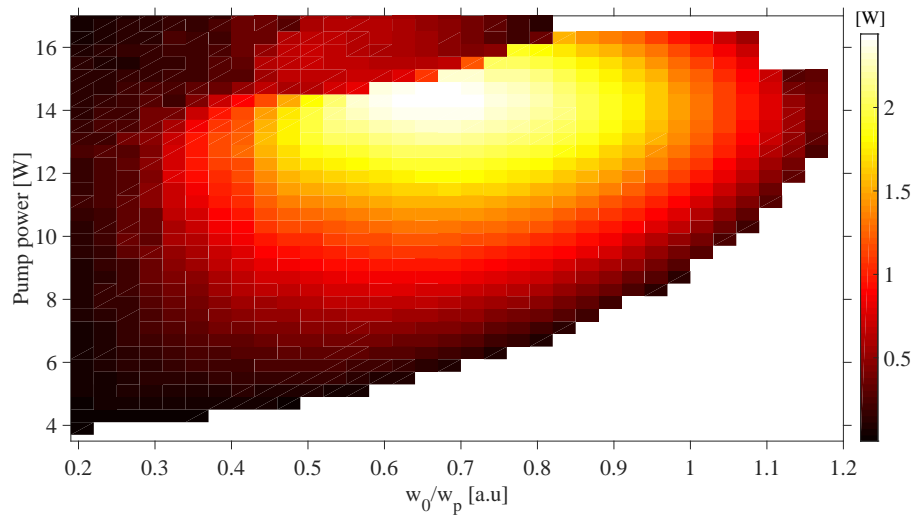


Figure 9. Simulated beam brightness after 15000 cavity round trips assuming a Gaussian pump shape. The solid blue line indicates the transition between multimode (left) and single mode operation (right).

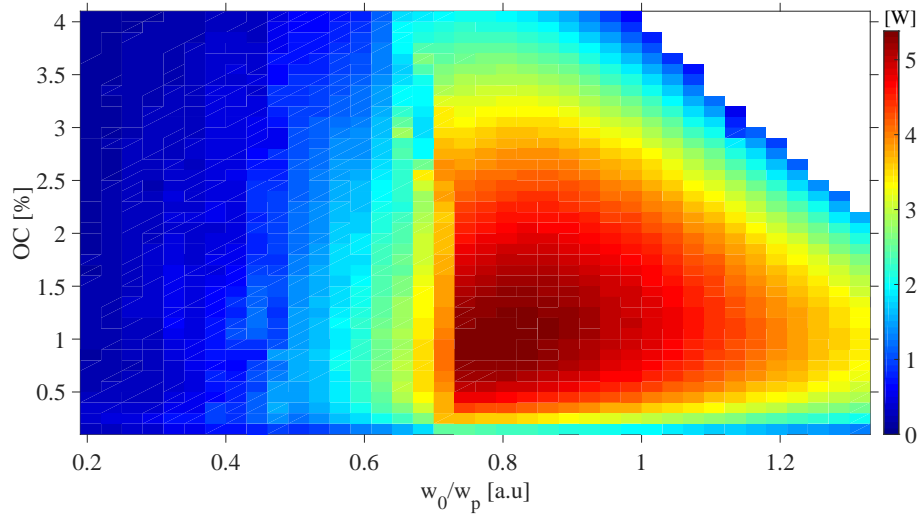


Figure 10. Simulated beam brightness after 15000 cavity round trips assuming a pump power of 19 W with a super-Gaussian beam shape.

The optimum output coupler for this structure and pump geometry is around 1%. This is in good agreement with experimental values obtained with AR-coated VECSEL structures.² This value is however expected to increase if the VECSEL structure is used as a folding mirror, or if the structure remains uncoated, as the modal gain per round trip will be higher. The optimum mode/pump size ratio remains around 0.82 for a super-Gaussian pump beam shape, independent of the OC losses. The sensitivity of the brightness to the mode ratio is also minimal at the optimum OC value of 1%, and is thus more forgiving when designing a VECSEL cavity.

5. CONCLUSION

We presented a system-oriented model to simulate the dynamics of transverse modes in VECSELs and conducted a parameter sweep to find optimum power and brightness values. The spatial gain profile was calculated taking into account the temperature distribution and the pump beam geometry, and an analytical expression was derived to compute the laser dynamics very efficiently. The transverse mode propagation and amplification was computed over thousands of round trips with a numerically optimized Huygens-Fresnel integral generalized to ABCD optical systems. We investigated the influence of the pump shape on the power performance and determined the optimum mode to pump size ratio for the highest laser brightness. Transitions between single and multimode operation were identified as a function of the mode size, pump power and output coupling losses, giving valuable insights for future design of VECSEL cavities.

Acknowledgments

This material is based upon work supported by the Air Force Office of Scientific Research under award number FA9550-17-1-0246. We would like to thank Robert Rockmore from the University of Arizona for helpful discussions.

REFERENCES

- [1] Heinen, B., Wang, T.-L., Sparenberg, M., Weber, A., Kunert, B., Hader, J., Koch, S., Moloney, J., Koch, M., and Stolz, W., “106 W continuous-wave output power from vertical-external-cavity surface-emitting laser,” *Electron. Lett* **48**(9), 516–517 (2012).
- [2] Laurain, A., Myara, M., Beaudoin, G., Sagnes, I., and Garnache, A., “Multiwatt-power highly-coherent compact single-frequency tunable vertical-external-cavity-surface-emitting-semiconductor-laser,” *Opt. Express* **18**(14), 14627–14636 (2010).
- [3] Zhang, F., Heinen, B., Wichmann, M., Möller, C., Kunert, B., Rahimi-Iman, A., Stolz, W., and Koch, M., “A 23-watt single-frequency vertical-external-cavity surface-emitting laser,” *Opt. Express* **22**, 12817–12822 (Jun 2014).
- [4] Laurain, A., Mart, C., Hader, J., Moloney, J. V., Kunert, B., and Stolz, W., “Optical noise of stabilized high-power single frequency optically pumped semiconductor laser,” *Opt. Lett.* **39**, 1573–1576 (Mar 2014).
- [5] Laurain, A., Mart, C., Hader, J., Moloney, J., Kunert, B., and Stolz, W., “15 W single frequency optically pumped semiconductor laser with sub-MHz linewidth,” *Photonics Technol. Lett. IEEE* **26**(2), 131–133 (2014).
- [6] Hader, J., Koch, S., and Moloney, J., “Microscopic theory of gain and spontaneous emission in gain laser material,” *Solid-State Electronics* **47**(3), 513–521 (2003).
- [7] Siegman, A. E., [*Lasers*], University Science Books, Mill Valley (California) (1986).
- [8] Laurain, A., Myara, M., Beaudoin, G., Sagnes, I., and Garnache, A., “High power single-frequency continuously-tunable compact extended-cavity semiconductor laser,” *Opt. Express* **17**(12), 9503–9508 (2009).
- [9] Siegman, A. E., Nemes, G., and Serna, J., “How to (maybe) measure laser beam quality,” in [*DPSS (Diode Pumped Solid State) Lasers: Applications and Issues*], *DPSS (Diode Pumped Solid State) Lasers: Applications and Issues*, MQ1, Optical Society of America (1998).
- [10] Wang, T., Kaneda, Y., Yarborough, J., Hader, J., Moloney, J., Chernikov, A., Chatterjee, S., Koch, S., Kunert, B., and Stolz, W., “High-power optically pumped semiconductor laser at 1040 nm,” *Photonics Technol. Lett. IEEE* **22**(9), 661–663 (2010).